

Initializing Decadal Climate Predictions with the GECCO Oceanic Synthesis: Effects on the North Atlantic

HOLGER POHLMANN* AND JOHANN H. JUNGCLAUS

Max-Planck-Institut für Meteorologie, Hamburg, Germany

ARMIN KÖHL AND DETLEF STAMMER

Institut für Meereskunde, Zentrum für Marine und Atmosphärische Wissenschaften, Universität Hamburg, Hamburg, Germany

JOCHEM MAROTZKE

Max-Planck-Institut für Meteorologie, Hamburg, Germany

(Manuscript received 18 March 2008, in final form 23 January 2009)

ABSTRACT

This study aims at improving the forecast skill of climate predictions through the use of ocean synthesis data for initial conditions of a coupled climate model. For this purpose, the coupled model of the Max Planck Institute (MPI) for Meteorology, which consists of the atmosphere model ECHAM5 and the MPI Ocean Model (MPI-OM), is initialized with oceanic synthesis fields available from the German contribution to Estimating the Circulation and Climate of the Ocean (GECCO) project. The use of an anomaly coupling scheme during the initialization avoids the main problems with drift in the climate predictions. Thus, the coupled model is continuously forced to follow the density anomalies of the GECCO synthesis over the period 1952–2001. Hindcast experiments are initialized from this experiment at constant intervals. The results show predictive skill through the initialization up to the decadal time scale, particularly over the North Atlantic. Viewed over the time scales analyzed here (annual, 5-yr, and 10-yr mean), greater skill for the North Atlantic sea surface temperature (SST) is obtained in the hindcast experiments than in either a damped persistence or trend forecast. The Atlantic meridional overturning circulation hindcast closely follows that of the GECCO oceanic synthesis. Hindcasts of global-mean temperature do not obtain greater skill than either damped persistence or a trend forecast, owing to the SST errors in the GECCO synthesis, outside the North Atlantic. An ensemble of forecast experiments is subsequently performed over the period 2002–11. North Atlantic SST from the forecast experiment agrees well with observations until the year 2007, and it is higher than if simulated without the oceanic initialization (averaged over the forecast period). The results confirm that both the initial and the boundary conditions must be accounted for in decadal climate predictions.

1. Introduction

This paper is concerned with climate predictions over interannual to decadal time scales, which stand in essential contrast to both seasonal climate predictions and century-long climate projections. Seasonal climate pre-

dictions with coupled atmosphere–ocean general circulation models (AOGCMs) are started from the observed recent climate state but have so far been performed using constant concentrations of greenhouse gases (GHGs) and aerosols, because the changes in the radiative forcing are assumed to occur slowly enough to be negligible on the seasonal time scale. Climate projections to the end of this century and beyond, such as those performed for the Fourth Assessment Report (AR4) of the Intergovernmental Panel on Climate Change (IPCC), obtain the changing radiative forcing from greenhouse gases and aerosols as essential input. The changing concentrations of greenhouse gases and aerosols are important not only for the longer but also

* Current affiliation: Met Office Hadley Centre, Exeter, United Kingdom.

Corresponding author address: Dr. Holger Pohlmann, Met Office Hadley Centre, FitzRoy Road, Exeter EX1 3PB, United Kingdom.
E-mail: holger.pohlmann@metoffice.gov.uk

for the decadal time scales (Lee et al. 2006; von Storch 2008). When inferring predictability from scenarios of the evolution of greenhouse gas and aerosol concentrations, one must consider that there are large differences between scenarios, which depend on assumed socioeconomic developments (e.g., Andreae et al. 2005).

Climate projections are not started from a state that reflects the best-known initial conditions; instead, they are started from a somewhat arbitrary point in time of a control integration. A chronology of the climate projection is established by specifying the time history of the concentrations of greenhouse gases and aerosols; hence, the initialization of the climate projection is assumed to represent somehow the climate of the mid-nineteenth century (ca. 1850). The model is then integrated into the present and future. In contrast to both seasonal climate prediction and climate projections, climate predictions over decadal time scales are expected to depend crucially on both the initial conditions and the changing radiative forcing (e.g., Cox and Stephenson 2007). Decadal climate predictions should therefore be started from the climate state of the recent past.

Predictability due to the initial conditions arises from the slow components of the climate system (see the recent overview by Collins 2007), most notably the ocean, although the presence of low-frequency climate variability is a necessary, but not sufficient, condition for climate predictability (Boer 2004; Pohlmann et al. 2004). Decadal climate predictability due to the oceanic initial conditions has been investigated in “perfect model” experiments. Predictability has been found over the ocean, particularly the North Atlantic, on the decadal time scale (Griffies and Bryan 1997; Pohlmann et al. 2004; Collins et al. 2006). However, these studies represent pure model results, without an inclusion of observations to define the initial climate conditions. In contrast, some recent work has employed initial conditions from observations. Troccoli and Palmer (2007) have initialized their model from an assimilation of full observations (as opposed to anomalies), which has introduced drift in their predictions from the observed toward an imperfect model climate. This problem can be reduced or overcome by initializing the climate predictions with anomalies rather than absolute values (Pierce et al. 2004; Smith et al. 2007; Keenlyside et al. 2008). However, implementing observed initial conditions into a coupled model that is incompatible with this state posed a serious problem. In the study of Pierce et al. (2004; see also Barnett et al. 2004), the model quickly “forgot” the details of the initial conditions because of model errors.

One factor that may limit climate predictability is caused by the lack of observations available for the

initialization of the climate models; even today, we do not have enough observations to create a dynamically balanced initial condition. We always need a synthesis process using data assimilation to create this balance; this statement also holds for the initialization of daily weather forecasts. Recent efforts in combining all available ocean observations into decadal oceanic syntheses of the time-varying ocean state (e.g., Stammer et al. 2002) offers new possibilities to improve the initialization of climate predictions and to estimate predictability by producing hindcast experiments (i.e., forecasts made retrospectively to assess the prediction skill of the system). Here, we use the results obtained by the German contribution to the Estimation of the Circulation and Climate of the Ocean (GECCO; Köhl and Stammer 2008a,b) project, which produces a dynamically and thermodynamically self-consistent description of the time-varying ocean state over the period 1952–2001. We use the GECCO synthesis as the oceanic initial conditions of our coupled climate model to assess the effect of the three-dimensional initialization on climate predictability.

The remainder of this paper is organized as follows: The AOGCM and the experiments are described in section 2. The methods used to identify predictability are introduced in section 3. The predictability results are presented in section 4. Discussion and conclusions are given in section 5.

2. Models and experiments

The global climate model used in this study is the European Centre-Hamburg model version 5–Max Planck Institute Ocean Model (ECHAM5–MPI-OM; Roeckner et al. 2003; Marsland et al. 2003) version Community Earth System Models (COSMOS)-1.0.0. The resolution is T63 L31 in the atmosphere and $1.5^\circ \times 1.5^\circ$ L40 in the ocean. The two components are coupled without flux adjustments or any other corrections. The model is an updated version of the Max Planck Institute for Meteorology IPCC AR4 model (Jungclaus et al. 2006) with optimization in the computational performance and user interface. The mean climate state in the updated model version is almost the same as before, but the variability is increased in some details because of small changes in the oceanic component. The climate model is described in more detail in the appendix.

The different experiments used in this study are summarized in Table 1. We have performed an ensemble of three twentieth-century (20C) simulations with observed GHG and tropospheric aerosol concentrations in the twentieth century and following the A1B scenario of the IPCC thereafter. The early period, until the year 1951, of

TABLE 1. Summary of experiments used in this study. Details are given in the text.

Expt	Initialization	Forcing	Amount	Period
20C	In 1900, 1910, and 1920 from an IPCC twentieth-century simulation	GHG + aerosol	3	1900, 1910, and 1920–2011
Assimilation	In 1952 from 20C (initialized in 1900)	GHG + aerosol and $T + S$ from GECCO	1	1952–2001
Hindcast	At the end of every year from assimilation	GHG + aerosol	49	10-yr duration
Forecast	At the end of assimilation	GHG + aerosol	7	2002–11

the 20C integrations is used as a spinup phase to allow the model to adjust to the parameter changes. The period of these experiments after 1951 is used to investigate the predictability resulting from the radiative forcing without the oceanic initialization.

An “assimilation run” is subsequently performed to provide the initial conditions for the hindcast experiments. During the assimilation run, monthly-mean temperature (T) and salinity (S) of the ocean component of the coupled model are relaxed toward the anomalies from the GECCO 1952–2001 synthesis (Köhl et al. 2007). GECCO builds on the first ECCO synthesis (Stammer et al. 2002) and uses a quasi-global configuration based on the Massachusetts Institute of Technology (MIT) ocean GCM (Marshall et al. 1997), with 1° horizontal resolution and 23 vertical levels. The GECCO framework uses the adjoint to the MIT GCM (Marotzke et al. 1999) to bring the model into consistency with available hydrographic and satellite data, as well as with prior estimates of surface fluxes of momentum, heat, and freshwater. The prior forcing fields consist of twice-daily wind stress and daily heat and freshwater flux fields from the National Centers for Environmental Prediction–National Center for Atmospheric Research (NCEP–NCAR) reanalysis (Kalnay et al. 1996). These forcing fields are adjusted every 10 days by the assimilation method to yield a model state that is dynamically consistent with the model physics and the assimilated data within given error limits.

The model error of the COSMOS model is shown as deviations of the surface air temperature (SAT) from a climatology (Jones et al. 1999) obtained from the Climate Research Unit (CRU) of the University of East Anglia over the period 1961–90 (Fig. 1); SAT error exceeds $\pm 3^\circ\text{C}$ in certain regions, which seems to be mostly related to the physical processes of sea ice cover and low-lying stratus cloud decks. If the forecasts were simply initialized with the full GECCO ocean synthesis, the errors of the coupled model would cause a drift in the system toward the mean state of the coupled model. To avoid this drift and an associated initial shock of the system, an anomaly coupling scheme similar to that of Pierce et al. (2004) is used. The monthly-mean GECCO

T and S anomalies are added to the mean state of the coupled model, and the ocean component of the coupled model is relaxed toward this combined state over the entire period 1952–2001. A linear interpolation is used to derive the intermonthly forcing fields. The relaxation time scale is 10 days. The anomaly coupling procedure is not performed in the top ocean model layer, which is covering the uppermost 7 m, or in regions where sea ice is present during the hindcast period. GECCO does not include a sea ice model and ends at 80°N ; regions that should form sea ice but do not, therefore exhibit an unphysical annual cycle, and we have to exclude the whole water column in the sea ice region and the region northward of 80°N from the anomaly coupling procedure. The oceanic surface layer is excluded from the anomaly coupling procedure to allow the surface and especially the sea ice in the coupled model to adjust to the atmospheric forcing.

Hindcast experiments are performed here over the period 1952–2001; one ensemble member is started at the end of every year from the assimilation experiment and run over 10 yr. This means that we allow the coupled system (atmosphere and ocean) to adjust dynamically to the GECCO ocean-state anomalies; the adjustment occurs over a period of 1–50 yr, depending on the start year. The resulting number of realizations is used to form an ensemble of 49 model runs.

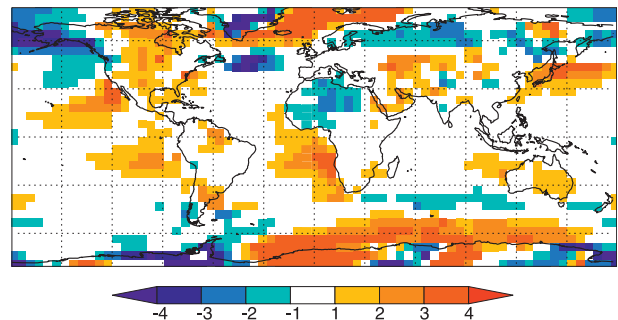


FIG. 1. SAT difference between the 20C integration and the CRU climatology for the annual means averaged over the period 1961–90.

3. Methods

We compare the hindcast results to sea surface temperature (SST) observations from the Hadley Centre Sea Ice and SST (HadISST; Rayner et al. 2003) dataset, SAT observations from the Hadley Centre Climatic Research Unit Temperature version 3 (HadCRUT3v; Brohan et al. 2006) dataset, and the GECCO synthesis. In this study, we are mainly analyzing the surface temperature and want to know if the predictions are skillful and, if they are, in which regions and for how long. Additionally, we compare the Atlantic meridional overturning circulation (MOC) of the hindcasts with that of the GECCO synthesis, providing an insight in the causes leading to the predictability.

We measure the skill of our system in terms of the anomaly correlation coefficient, COR:

$$\text{COR}(t) = \frac{\sum_{i=1}^n [x_i(t) - \bar{x}][o(i+t) - \bar{o}]}{\sqrt{\sum_{i=1}^n [x_i(t) - \bar{x}]^2 \sum_{i=1}^n [o(i+t) - \bar{o}]^2}}, \quad (1)$$

where x_i is the i th hindcast experiment, starting at the end of year (1951 + i); o is the observation or the GECCO data; t is the lead time; and n is the ensemble size. The overbar denotes time averages over the analyzed period 1952–2001, which is chosen to be the same for the observations and the GECCO data. We apply this measure of skill to each grid point and to regional and global averages. The significance of COR is estimated based on a t test. Additionally, the 20C experiments are compared with observations. We do not expect any predictive skill in the 20C experiments on the shorter time scales; however, on the longer time scales, these experiments can be used to estimate the climate change signal that is due to boundary forcing.

We obtain another quantitative assessment of the role of initialization through anomaly coupling by comparing the skill of the coupled model with the skill of damped persistence and trend predictions. Damped persistence predictions are started from observations with their extrapolations damped toward the climatological mean state. Therefore, the damping constant is calculated as the lag-1 autocorrelation coefficient from the observations and (for the forecast)¹ the climatological mean is

¹ Because we are using the anomaly correlation coefficient to estimate the skill of our hindcast experiments, the results obtained with this method are independent of the value of the climatological mean. Moreover, it can be shown that the anomaly correlation coefficient of the damped persistence hindcasts is equivalent to the lag autocorrelation coefficient of the observations.

defined as the mean over the period 1952–2001. Similarly, for the trend prediction, simply the trend calculated from the prior year (or pentad or decade) to the initial year (or pentad or decade) is extrapolated into the future using data between 1952 and 2001. At this point, we would like to advise the reader that we use the term pentadal (decadal) mean as the average over any 5 (10)-yr period.

4. Results

We obtain an overview of the regions with the highest predictability from the regional distribution of the anomaly correlation coefficients for SAT (SAT COR; Fig. 2) and SST (SST COR; Fig. 3). In general, SAT COR is low over land. In the 20C experiment, SAT COR is significant over the Indian Ocean, which mainly results from the correct simulation of the upward trend in the 20C experiment. In the hindcast experiment, the SAT COR with the observations is significant in the first year over the western Pacific and the North Atlantic. The most interesting feature of the SAT COR distribution is that a pattern with high correlation values remains significant on the decadal time scale over parts of the North Atlantic and the Mediterranean Sea (Figs. 2c,d). In the 20C experiment, the SST COR with the GECCO data is significant only in limited areas (Fig. 3a). In the hindcast experiment, however, the SST COR is significant in the first year over wide areas of the ocean (Fig. 3b) with exceptions in the Indian Ocean and some other regions. Similar to the SAT COR, a pattern with high correlation values remains significant over parts of the North Atlantic and the Mediterranean Sea (Figs. 3c,d). Other regions with long-term predictability exist over the tropical west Pacific.

The high SST COR values over the North Atlantic motivate us to analyze the time series of an index of North Atlantic SST. The North Atlantic SST index is defined as the area average over the region 0°–60°N, 50°–10°W (Fig. 4). The ensemble-mean 20C simulation has a negative temperature bias of 0.24 K compared to observations from the HadISST dataset (Rayner et al. 2003) over the North Atlantic region during the period 1952–2001. In Fig. 4, the temperature bias is removed by adding 0.24 K to every climate simulation with ECHAM5–MPI-OM. Similarly, a smaller SST bias of 0.05 K is removed from the GECCO data. The North Atlantic SST COR between the GECCO data and the hindcast experiments is significant up to the decadal time scale. Analyzing pentadal and decadal means makes it even more obvious that the hindcast experiments follow the GECCO experiment and observations more closely than the ensemble-mean 20C experiment does. When the SST COR is calculated between the hindcasts and the

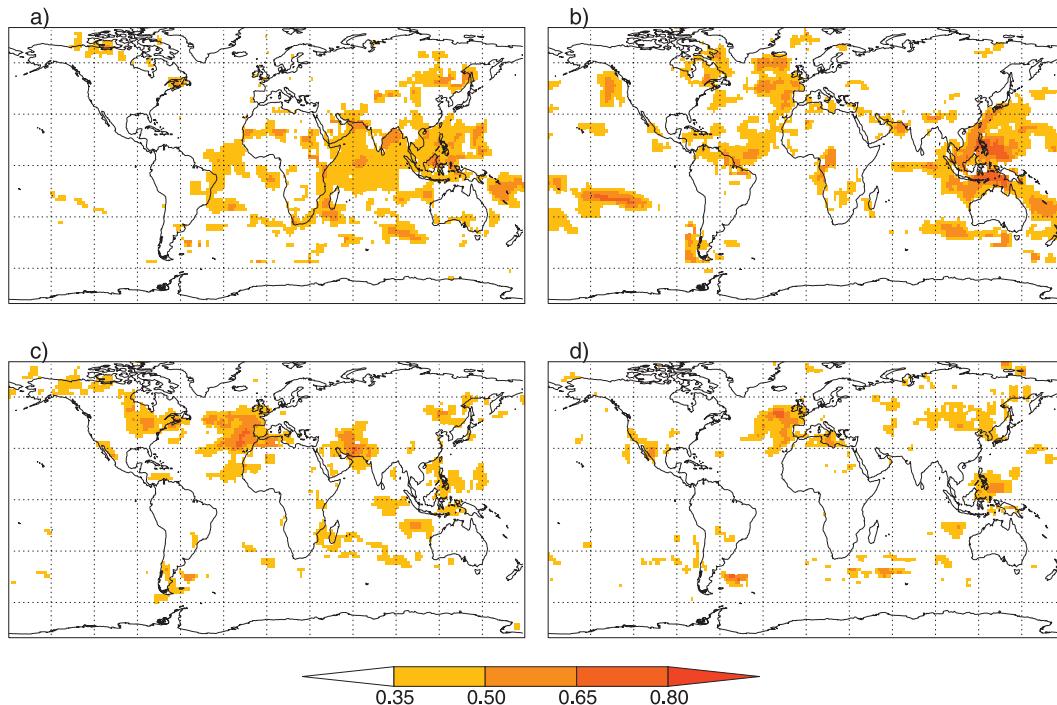


FIG. 2. SAT COR between the observations from the HadCRUT3v dataset and the following: (a) the ensemble-mean 20C experiment and the hindcasts for (b) the first year, (c) year 5, and (d) year 10. The colored areas are significant at the 95% level according to a t test.

observations, instead of between hindcasts and GECCO results, the correlation values are generally reduced, dropping below the significance limit for decadal means. The damped persistence forecast reaches correlation values as high as the SST COR from the hindcast experiment on the shorter time scales (up to three years), and the trend forecast reaches correlation values as high as the SST COR from the hindcast experiment for the decadal means. Both statistical methods are clearly inferior to the hindcast experiments on the 5-yr time scale. Viewed over all time scales, our hindcast experiments produce greater skill than damped persistence or the trend forecast.

The potential predictability of the Atlantic MOC in perfect model experiments with ECHAM5-MPI-OM (Pohlmann et al. 2004) motivates us to also analyze the predictability of the Atlantic MOC in our experiments. Owing to a lack of continuous MOC observations prior to 2004 (Cunningham et al. 2007; Kanzow et al. 2007), we assess MOC predictability by comparing to the MOC from the GECCO synthesis. We first note that the structure of the Atlantic MOC is different between the ECHAM5-MPI-OM and GECCO models; the maximum of the Atlantic MOC occurs at 35°N in the ECHAM5-MPI-OM 20C experiment, whereas it is located at 48°N in the GECCO results. The maximum Atlantic MOC at

48°N of the assimilation experiment agrees well with that of the GECCO estimate; the correlation coefficient is 0.81 in the case of annual means and even higher in the cases of pentadal and decadal means (0.93 and 0.97, respectively). On the other hand, the MOC variability in the ensemble-mean 20C experiment does not correspond to the MOC variability of the GECCO synthesis; the correlation coefficient between the 20C experiment and the GECCO synthesis is negative over the period 1952–2001 (Fig. 5). This lack of correlation is not surprising for the year-to-year and even longer-term variabilities, which the 20C experiment is not designed to reproduce. In contrast, the hindcast experiment and the GECCO synthesis show close correspondence in the low-frequency variability of the Atlantic MOC at 48°N (Fig. 5), demonstrating that the initial conditions of the hindcast experiments contain important information about the evolution of the MOC. At latitudes other than 48°N, there is less agreement of the Atlantic MOC between the assimilation and the GECCO synthesis (not shown). Also, the anomaly correlation coefficient between the hindcast and GECCO shows a rapid decline of forecast skill for lead times beyond 6 yr (Fig. 5), in marked contrast to the skill for North Atlantic SST where the decline with lead time is slower (Fig. 4). When we compare the hindcast experiments to the statistical

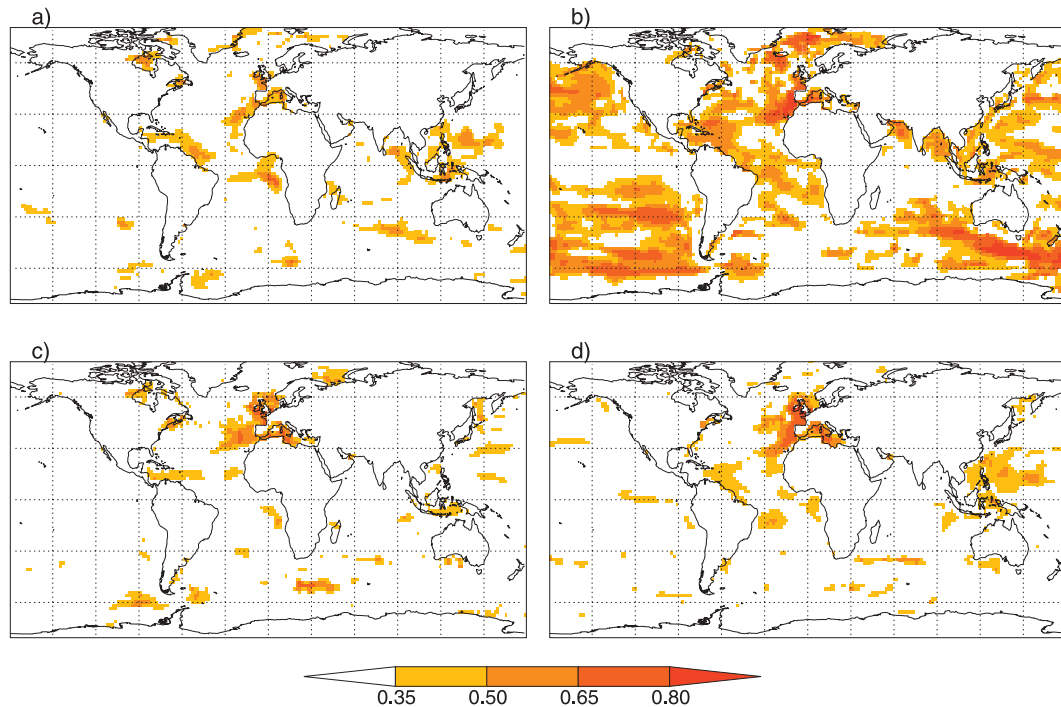


FIG. 3. SST COR between the GECCO data and the following: (a) the ensemble-mean 20C experiment and the hindcasts for (b) the first year, (c) year 5, and (d) year 10. The colored areas are significant at the 95% level according to a t test.

prediction methods in their ability to match the GECCO Atlantic MOC at 48°N , we find little difference for lead times of 1–3 yr and inferior skill of the hindcasts for lead times of 8–10 yr. As seen for the North Atlantic SST, however, the hindcast experiments show an advantage over the damped persistence and trend forecast on the intermediate time scales.

We expect a physical connection between North Atlantic MOC and SST, yet the differences in predictability require explanation. A lag-correlation analysis shows that the Atlantic MOC leads the North Atlantic SST index in the assimilation experiment; a significant maximum is present at about 5 yr (Fig. 6). This lag of 5 yr is consistent with the findings in century-long simulations with constant GHG and aerosol forcing (Latif et al. 2004); the Atlantic MOC fluctuations go along with oceanic heat transport fluctuations, which affect the climate in the North Atlantic region (Pohlmann et al. 2006). We may speculate that the MOC as reflected in the initial conditions carries within it the “memory” of the time history of roughly the past 5 yr and permits predictability of SST over 5 yr into the future. A predictability window for the MOC of about 5 yr would then imply SST predictability over 10 yr, consistent with Fig. 4.

In a next step, we analyze the predictability of the globally averaged SST (Fig. 7). The temperature bias of

0.01 K between the 20C experiment and the HadISST observations is removed in all ECHAM5–MPI-OM simulations, and a bias of 0.31 K is removed from the GECCO synthesis. The global-mean SST COR is generally lower when the hindcast experiments are compared to observations instead of the GECCO synthesis; at no lead time does the COR of the hindcasts with the observations significantly exceed the COR of the 20C experiment with observations. The relatively low COR of the hindcasts with the observations is caused by the relatively large disagreements between the GECCO synthesis and observations, which lead to inaccurate initial conditions for the hindcast experiments. A more-detailed comparison of regional temperature trends (not shown) indicates that the discrepancy between the global means of HadISST and GECCO SST arises mainly because GECCO SST is too high in the Southern Hemisphere in the 1950s, too low in the Pacific in the 1970s, and too high in the Pacific in the 1990s. For the global-mean SST, the damped persistence forecast shows predictive skill that is on all time scales in the range of the hindcast experiments, and on the decadal time scales the 20C experiment and the trend forecast also have high SST COR values, which means that much of the predictive skill is due to changes in the boundary conditions.

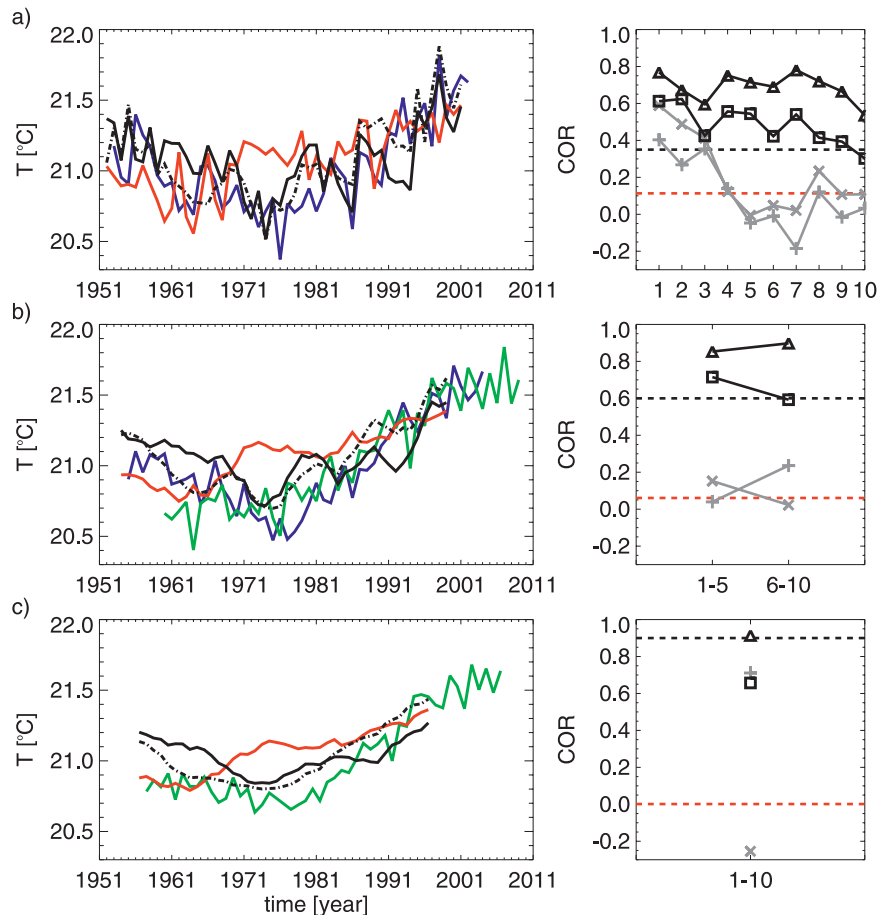


FIG. 4. (top left) Time series of North Atlantic annual-mean SST ($^{\circ}\text{C}$) averaged over the region 0° – 60°N , 50° – 10°W from the observations (HadISST; solid black), GECCO (dashed-dotted black), hindcast for the first prediction year (blue), and ensemble-mean 20C experiment (red). (top right) Anomaly correlation coefficient between the hindcast and the observations (squares) and between the hindcast and GECCO (triangles), with the anomaly correlation coefficient between the 20C experiment and observations (dashed red), the 95% significance level (dashed black), and the damped persistence (crosses) and trend (plus) predictions. (middle) As in (top), but for pentadal running means. The first (blue) and second (green) pentads are shown from the hindcast experiment. (bottom) As in (top), but for decadal running means. Decadal means (green) are shown from the hindcast experiment. All experimental data are bias corrected.

Encouraged by the decadal predictability shown through our hindcast experiments, we start an ensemble of seven forecast experiments from the assimilation experiment in the year 2002, the last year of the assimilation experiment, by perturbing the atmospheric horizontal diffusion coefficient by a small amount (on the order of $10^{-3}\%$). Averaged over the period 2002–07, the SAT is significantly higher in the forecast experiment ensemble mean than in the 20C experiment over North America, Europe, and parts of the North Atlantic (Fig. 8). The differences over the North Atlantic let us analyze an index for the North Atlantic SST in more detail (Fig. 9). We estimate the significance of the dif-

ference between the observation and the experiments by assuming the ensemble to be Gauss distributed. If the observation at a certain time falls in the range of 1.6 standard deviations (90%) around the ensemble mean, we assume the experiment to be close to the observation. With this definition, the forecast experiment is close to the observation over the whole period 2002–07, in contrast to the 20C experiment, which is different to the observations after the third prediction year (Fig. 9a). For the period 2002–06, the forecast ensemble mean is closer to the observations than the 20C ensemble mean and the statistical forecasts (Fig. 9b). For the periods 2007–11 (Fig. 9b) and 2002–11 (Fig. 9c), the North

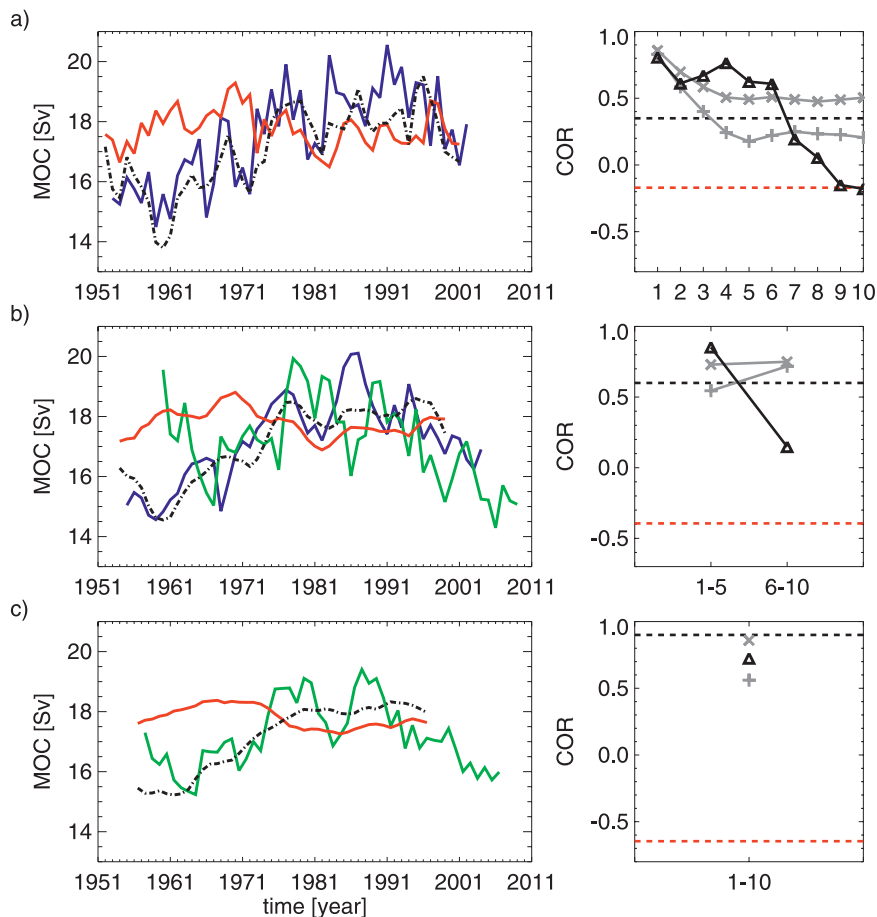


FIG. 5. (top left) Time series of the maximum of the annual-mean Atlantic MOC [Sv ($1 \text{ Sv} \equiv 10^6 \text{ m}^3 \text{ s}^{-1}$)] at 48°N from GECCO (dashed-dotted black), hindcast for the first prediction year (blue), and ensemble-mean 20C experiment (red). (top right) Anomaly correlation coefficient between the hindcast and the GECCO experiments (triangles), together with the anomaly correlation coefficient between the 20C experiment and observations (dashed black), the 95% significance level (dashed black), and the damped persistence (crosses) and trend (plus) predictions. (middle) As in (top), but for pentadal running means. The first (blue) and second (green) pentads are shown from the hindcast experiment. (bottom) As in (top), but for decadal running means. Decadal means (green) are shown from the hindcast experiment.

Atlantic SST is predicted to remain almost constant by the forecast ensemble with respect to the period 2002–06, whereas an increase is predicted by the trend forecast and a decrease is predicted by the 20C ensemble and the damped persistence forecast.

5. Summary and discussion

We have initialized the coupled model ECHAM5–MPI-OM with oceanic synthesis results from the GECCO project. The assimilation run is continuously forced to follow the density anomalies of the GECCO ocean synthesis over the period 1952–2001. The hindcast experiments are started from this assimilation run at constant

intervals. The anomaly coupling scheme avoids the main problems with drift in the hindcast experiments. However, because of this procedure, the forecast products are contaminated by the climate model biases, which must be removed afterward.

Our results show predictive skill up to the decadal time scales for the North Atlantic SST, in contrast to the 20C experiment. In terms of the anomaly correlation coefficient, the retrospective predictions are superior to both the damped persistence and the trend forecast on the intermediate time scale. On the decadal time scale, the high prediction skill of the trend forecast shows that much of the decadal signal is due to the boundary forcing. However, one caveat of this result lies in the fact that

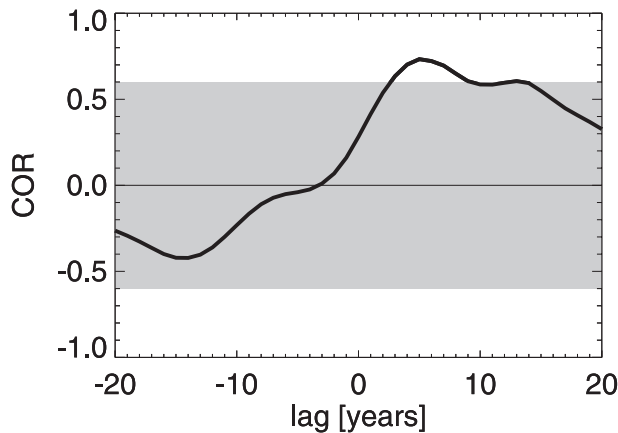


FIG. 6. Cross correlation of the North Atlantic SST averaged over the region 0° – 60° N, 50° – 10° W and maximum Atlantic MOC at 48° N for 5-yr running means from the assimilation experiment, with the range indicating less than 95% significance (shaded gray) according to a t test. Maximum correlation is found at positive time lags, which indicates that the Atlantic MOC leads the North Atlantic SST.

the predictive skill is mainly due to the low North Atlantic SST in the early 1970s. Without such a feature in the future, the predictive skill of North Atlantic climate might be overestimated in this study.

Predictability is also found for the Atlantic MOC at 48° N, where the long-term trend of the MOC in the assimilation run closely follows the GECCO synthesis. But at other latitudes, the Atlantic MOC of the assimilation run develops quite independently of the GECCO results, suggesting that predictive skill for the MOC might be limited to high latitudes, where a clear relation has been demonstrated between the past North Atlantic Oscillation and the MOC strength (Eden and Willebrand 2001). In contrast, the MOC around 25° N is strongly influenced by Rossby waves (Köhl 2005; Hirschi et al. 2007; Köhl and Stammer 2008b), which would not be predictable, especially when baroclinically unstable (Köhl 2005; Köhl and Stammer 2008b). The lagged correlation analysis between the Atlantic MOC and SST indices shows a maximum correlation with

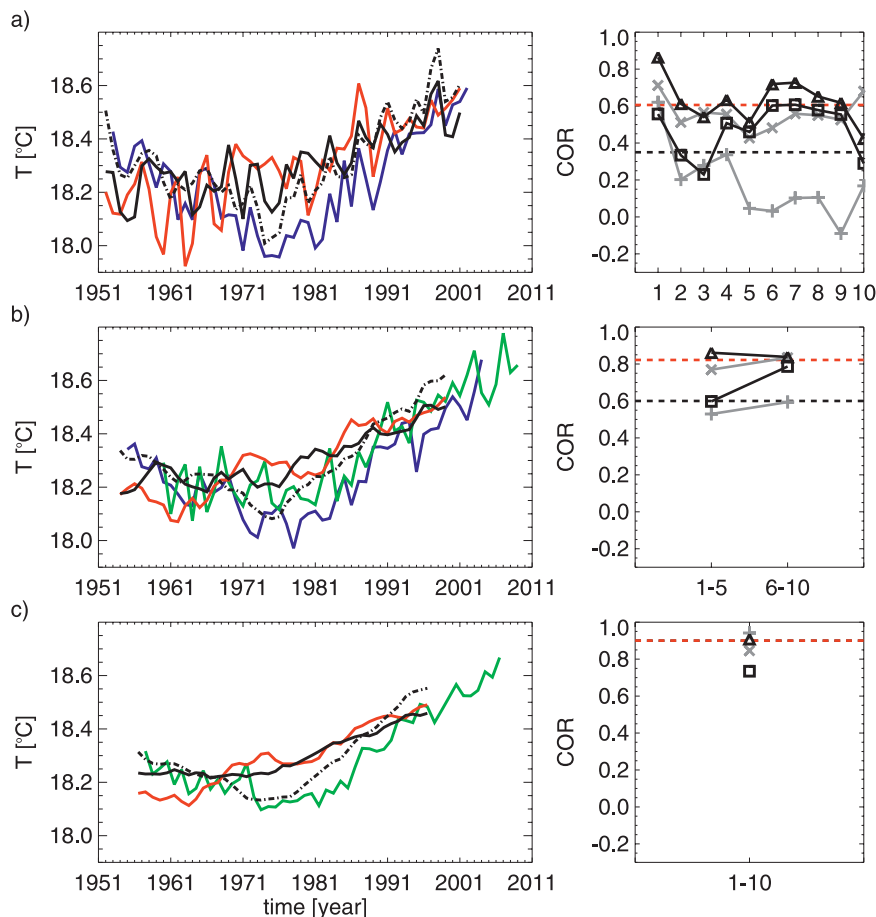


FIG. 7. Same as Fig. 4, but the time series of mean SST are globally averaged.

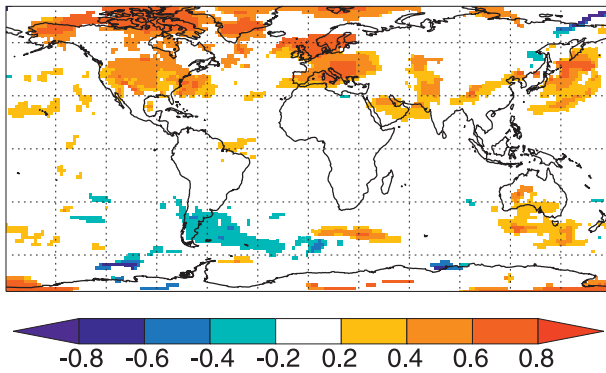


FIG. 8. Difference between the SAT (K) of the forecast and the 20C experiments averaged over the period 2002–07. The colored areas are significant at the 90% level according to a t test.

MOC leading by about 5 yr. That the Atlantic MOC leads the North Atlantic SST variability hints at an influence of the former on the latter. A lag of a few years between the Atlantic MOC and the North Atlantic SST was also found in a multicentury control experiment with ECHAM5–MPI-OM (Latif et al. 2004). However, because there are not enough observations of the Atlantic MOC variability, it is not yet clear how realistically the MOC is reproduced in the GECCO synthesis.

When we compare the hindcasts to observations rather than to the GECCO data, the SST COR is generally reduced. This problem arises because the GECCO optimization procedure permits an SST error of ± 1 K, which is quite large and leads to inaccurate initial conditions for the climate predictions. Combining the initialization of the climate prediction system with data from the GECCO synthesis (for the subsurface ocean) and SST and sea ice observations (for the ocean surface) could therefore reduce the forecast errors.

This procedure of combining the initialization of the prediction system with GECCO synthesis for the subsurface ocean and SST and sea ice observations for the surface would also eliminate the problem of drift in the Atlantic MOC, which is present when the climate model is initialized with SST data only (Keenlyside et al. 2008). The advections of temperature and salinity anomalies at the ocean surface tend to compensate each other. Because Keenlyside et al. (2008) only used SST restoring, the sea surface salinity (SSS) was free to adjust independently. The different adjustment times of SST and SSS meant that the density compensation could not take place to a realistic extent, which caused the unrealistic densities. This problem is not present in our study, because a restoring of both temperature and salinity is used. However, we anticipate that, ultimately, a system that uses the same model for the data synthesis and forecasts will lead to the best forecast results.

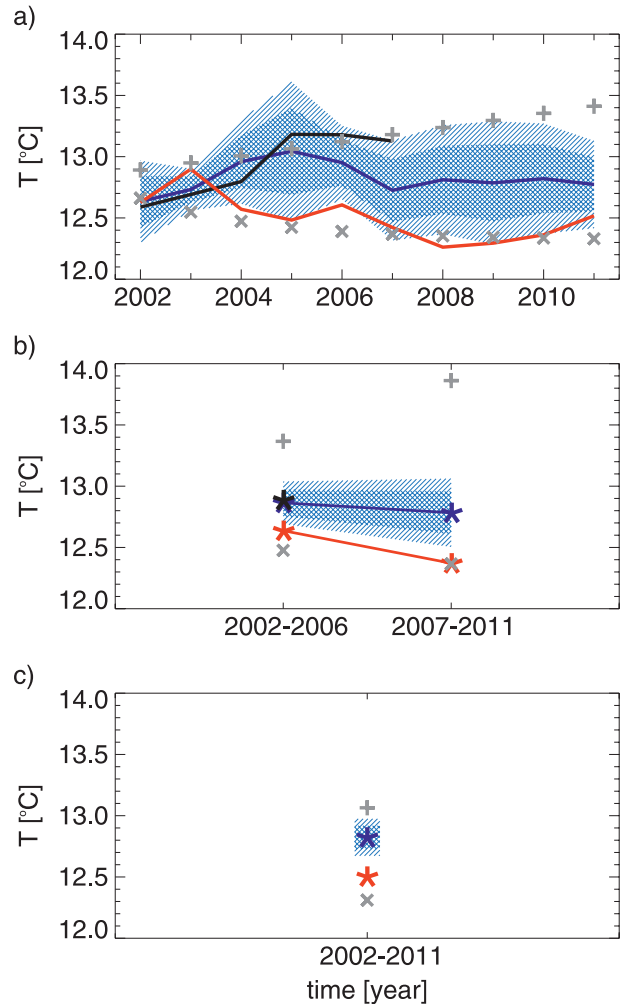


FIG. 9. (a) Annual-mean North Atlantic SST ($^{\circ}\text{C}$) averaged over the region 40° – 60°N , 50° – 10°W of observations (HadISST; black), the ensemble-mean 20C (red) and forecast (blue) experiments, together with the damped persistence and trend (plus) predictions. The light (dark) shading represents the 90% (70%) range of the forecast ensemble. (b),(c) As in (a), but for (b) 5-yr and (c) 10-yr means. The North Atlantic SST data from the experiments are bias corrected.

We have demonstrated the applicability of our prediction system with a decadal forecast experiment initialized from the assimilation run in the year 2002. The predicted North Atlantic SST is higher than without the initialization and, it is, on average, much closer to observations than in the 20C experiment, until the year 2007. Averaged over the period 2002–07, the SAT is considerably higher than without the initialization in large parts of the Northern Hemisphere, with an extension also over the continents. Here, we describe only the first attempt at decadal prediction with our coupled model combined with the GECCO synthesis, but all indications are that we should pursue this approach

further. Furthermore, the recent increase in the number of subsurface ocean observations, especially through the Argo project (Roemmich and Owens 2000), should improve our ability to initialize the oceanic state for more accurate climate predictions.

Acknowledgments. We thank Drs. Daniela Matei, Uwe Mikolajewicz, and Jin-Song von Storch for the discussion of our results and comments on this paper. The comments by two anonymous reviewers were very helpful in improving the manuscript. This work was supported in part by the German Ministry for Education and Research (BMBF) project The North Atlantic as Part of the Earth System: From System Comprehension to Analysis of Regional Impacts (Contract 03F0443E). The climate simulations were performed at the German Climate Computing Centre (DKRZ). We used observational surface air temperature data representing a climatology over the period 1961–90 obtained from the Climatic Research Unit of the University of East Anglia (available online at <http://www.cru.uea.ac.uk>), surface air temperature data from the HadCRUT3v, and sea surface temperature data from the HadISST dataset of the Met Office Hadley Centre (available online at <http://hadobs.metoffice.com>).

APPENDIX

Model Description

The coupled model ECHAM5–MPI-OM consists of the atmosphere component ECHAM5 and the ocean–sea ice model MPI-OM. In the atmosphere model (Roeckner et al. 2003), vorticity, divergence, temperature, and the logarithm of surface pressure are represented by a truncated series of spherical harmonics with triangular truncation 63 (T63), whereas the advection of water vapor, cloud liquid water, and cloud ice is treated by a flux-form semi-Lagrangian scheme. A hybrid sigma–pressure system is used in the vertical direction (31 layers with the top model level at 10 hPa). The model uses state-of-the-art parameterizations for shortwave and longwave radiation, stratiform clouds, cumulus convection, boundary layer and land surface processes, and gravity wave drag.

The well-mixed greenhouse gases (CO_2 , CH_4 , N_2O , F11*, and F12) are prescribed as annual global means according to observations (fit to ice core data and direct observations), in which F11* also includes the effect of the minor halocarbons. Monthly data of stratospheric and tropospheric ozone concentrations are prescribed as two-dimensional (latitude and height) distributions

(Kiehl et al. 1999). The spatiotemporal distribution of sulfate aerosols is prescribed using the respective data from an offline simulation (Boucher and Pham 2002). Both the direct and first indirect (cloud albedo) effects of sulfate are included.

A mass flux scheme for shallow, midlevel, and deep convection (Tiedtke 1989) is applied with modifications for deep convection according to Nordeng (1994). The scheme is based on steady-state equations for mass, heat, moisture, cloud water, and momentum for an ensemble of updrafts and downdrafts, including turbulent and organized entrainment and detrainment. Cloud water detrainment in the upper part of the convective updrafts is used as a source term in the stratiform cloud water equations. For deep convection, an adjustment-type closure is used with convective activity expressed in terms of convective available potential energy.

An implicit scheme is used for coupling the land surface and the atmosphere (Schulz et al. 2001). Also, the heat transfer in the soil is calculated by using an implicit scheme. In the presence of snow, the top of the snow layer is considered as the top of the soil model. The heat conductivity is modified accordingly in all layers that are totally or partially filled with snow. A prognostic equation for the amount of snow on the canopy has been introduced. Snow changes on the canopy result from interception of snowfall, sublimation, melting, and unloading resulting from wind (Roesch et al. 2001). The grid-mean surface albedo depends on the specified background albedo, a specified snow albedo (function of temperature), the area of the grid cell covered with forest, the snow cover on the ground (function of snow depth and slope of terrain), and the snow cover on the canopy (Roesch et al. 2001). A new set of land surface data (vegetation ratio, leaf area index, forest ratio, and background albedo) has been derived from a global 1-km-resolution dataset (Hagemann 2002).

Technical details of the ocean model MPI-OM, the embedded sea ice model, and the parameterizations that have been implemented during the transition from the Hamburg Ocean Primitive Equation (HOPE) model (Wolff et al. 1997) to the MPI-OM model can be found in Marsland et al. (2003). Here, we summarize the main features.

The primitive equations for a hydrostatic Boussinesq fluid are formulated with a free surface. The vertical discretization is on z levels, and the bottom topography is resolved by way of partial grid cells (Wolff et al. 1997). The spatial arrangement of scalar and vector variables is formulated on a C grid (Arakawa and Lamb 1977). The along-isopycnal diffusion follows Redi (1982) and Griffies (1998). Isopycnal tracer mixing by unresolved eddies is parameterized following Gent et al. (1995). For

the vertical eddy viscosity and diffusion, the Richardson number–dependent scheme of Pacanowski and Philander (1981, hereafter PP) is applied. Because the PP scheme in its classical form underestimates the turbulent mixing close to the surface, an additional wind mixing is included that is proportional to the cube of the 10-m wind speed and decays exponentially with depth. In the presence of static instability, convective overturning is parameterized by greatly enhanced vertical diffusion. A slope convection scheme has been included that allows for a better representation of the flow of statically unstable dense water over sills (e.g., the Denmark Strait and the Strait of Gibraltar; for details, see Marsland et al. 2003) and off shelves (e.g., the Arctic and Antarctic shelves).

The dynamics of sea ice are formulated using viscous–plastic rheology (Hibler 1979). The thermodynamics relate changes in sea ice thickness to a balance of radiant, turbulent, and oceanic heat fluxes. The effect of snow accumulation on sea ice is included, along with snow–ice transformation when the snow–ice interface sinks below the sea level because of snow loading. The effect of ice formation and melting is accounted for within the model, assuming a sea ice salinity of 5 psu.

REFERENCES

- Andreae, M. O., C. D. Jones, and P. M. Cox, 2005: Strong present-day cooling implies a hot future. *Nature*, **435**, 1187–1190.
- Arakawa, A., and V. R. Lamb, 1977: Computational design of the basic dynamical processes of the UCLA general circulation model. *Methods Comput. Phys.*, **17**, 173–265.
- Barnett, T., R. Malone, W. Pennell, D. Stammer, B. Semtner, and W. Washington, 2004: The effects of climate change on water resources in the west: Introduction and overview. *Climatic Change*, **62**, 1–11.
- Boer, G. J., 2004: Long time-scale potential predictability in an ensemble of coupled climate models. *Climate Dyn.*, **23**, 29–44.
- Boucher, O., and M. Pham, 2002: History of sulfate aerosol radiative forcings. *Geophys. Res. Lett.*, **29**, 1308, doi:10.1029/2001GL014048.
- Brohan, P., J. J. Kennedy, I. Harris, S. F. B. Tett, and P. D. Jones, 2006: Uncertainty estimates in regional and global observed temperature changes: A new data set from 1850. *J. Geophys. Res.*, **111**, D12106, doi:10.1029/2005JD006548.
- Collins, M., 2007: Ensembles and probabilities: A new era in the prediction of climate change. *Phil. Trans. Roy. Soc.*, **365A**, 1957–1970.
- , and Coauthors, 2006: Interannual to decadal climate predictability in the North Atlantic: A multimodel-ensemble study. *J. Climate*, **19**, 1195–1203.
- Cox, P., and D. Stephenson, 2007: A changing climate for prediction. *Science*, **317**, 207–208.
- Cunningham, S. A., and Coauthors, 2007: Temporal variability of the Atlantic meridional overturning circulation at 26.5°N. *Science*, **317**, 935–938.
- Eden, C., and J. Willebrand, 2001: Mechanism of interannual to decadal variability of the North Atlantic Circulation. *J. Climate*, **14**, 2266–2280.
- Gent, P. R., J. Willebrand, T. McDougall, and J. C. McWilliams, 1995: Parameterizing eddy-induced tracer transports in ocean circulation models. *J. Phys. Oceanogr.*, **25**, 463–474.
- Griffies, S. M., 1998: The Gent–McWilliams skew flux. *J. Phys. Oceanogr.*, **28**, 831–841.
- , and K. Bryan, 1997: Predictability of the North Atlantic multidecadal climate variability. *Science*, **275**, 181–184.
- Hagemann, S., 2002: An improved land surface parameter data set for global and regional climate models. Max-Planck-Institut für Meteorologie Rep. 336, 28 pp.
- Hibler, W. D., III, 1979: A dynamic thermodynamic sea ice model. *J. Phys. Oceanogr.*, **9**, 815–846.
- Hirschi, J. J. M., P. D. Killworth, and J. R. Blundell, 2007: Sub-annual, seasonal, and interannual variability of the North Atlantic meridional overturning circulation. *J. Phys. Oceanogr.*, **37**, 1246–1265.
- Jones, P. D., M. New, D. E. Parker, S. Martin, and I. G. Rigor, 1999: Surface air temperature and its variations over the last 150 years. *Rev. Geophys.*, **37**, 173–199.
- Jungclaus, J. H., and Coauthors, 2006: Ocean circulation and tropical variability in the coupled Model ECHAM5/MPI-OM. *J. Climate*, **19**, 3952–3972.
- Kalnay, E., and Coauthors, 1996: The NCEP/NCAR 40-Year Reanalysis Project. *Bull. Amer. Meteor. Soc.*, **77**, 437–471.
- Kanzow, T., and Coauthors, 2007: Observed flow compensation associated with the MOC at 26.5°N in the Atlantic. *Science*, **317**, 938–941.
- Keenlyside, N. S., M. Latif, J. Jungclaus, L. Kornbluh, and E. Roeckner, 2008: Advancing decadal-scale climate prediction in the North Atlantic sector. *Nature*, **453**, 84–88, doi:10.1038/nature06921.
- Kiehl, J. T., T. Schneider, R. Portman, and S. Solomon, 1999: Climate forcing due to tropospheric and stratospheric ozone. *J. Geophys. Res.*, **104**, 31 239–31 254.
- Köhl, A., 2005: Anomalies of meridional overturning: Mechanisms in the North Atlantic. *J. Phys. Oceanogr.*, **35**, 1455–1472.
- , and D. Stammer, 2008a: Decadal sea level changes in the 50-Year GECCO ocean synthesis. *J. Climate*, **21**, 1876–1890.
- , and —, 2008b: Variability of the meridional overturning in the North Atlantic from the 50 years GECCO state estimation. *J. Phys. Oceanogr.*, **38**, 1913–1930.
- , —, and B. Cornuelle, 2007: Interannual to decadal changes in the ECCO global synthesis. *J. Phys. Oceanogr.*, **37**, 313–337.
- Latif, M., and Coauthors, 2004: Reconstructing, monitoring, and predicting multidecadal-scale changes in the North Atlantic thermohaline circulation with sea surface temperature. *J. Climate*, **17**, 1605–1614.
- Lee, T. C. K., F. C. Zwiers, X. Zhang, and M. Tsao, 2006: Evidence of decadal prediction skill resulting from changes in anthropogenic forcing. *J. Climate*, **19**, 5305–5318.
- Marotzke, J., R. Giering, K. Q. Zhang, D. Stammer, C. Hill, and T. Lee, 1999: Construction of the adjoint MIT ocean general circulation model and application to Atlantic heat transport sensitivity. *J. Geophys. Res.*, **104**, 29 529–29 548.
- Marshall, J., A. Adcroft, C. Hill, L. Perelman, and C. Heisey, 1997: A finite-volume, incompressible Navier–Stokes model for studies of the ocean on parallel computers. *J. Geophys. Res.*, **102** (C3), 5753–5766.
- Marsland, S. J., H. Haak, J. H. Jungclaus, M. Latif, and F. Röske, 2003: The Max-Planck-Institute global ocean/sea ice model with orthogonal curvilinear coordinates. *Ocean Modell.*, **5**, 91–127.
- Nordeng, T. E., 1994: Extended versions of the convective parameterization scheme at ECMWF and their impact on the

- mean and transient activity of the model in the tropics. ECMWF Tech. Memo. 206, 42 pp.
- Pacanowski, R. C., and S. G. H. Philander, 1981: Parameterization of vertical mixing in numerical models of tropical oceans. *J. Phys. Oceanogr.*, **11**, 1443–1451.
- Pierce, D. W., T. P. Barnett, R. Tokmakian, A. Semtner, M. Maltrud, J. Lysne, and A. Craig, 2004: The ACPI project, element 1: Initializing a coupled climate model from observed conditions. *Climatic Change*, **62**, 13–28.
- Pohlmann, H., M. Botzet, M. Latif, A. Roesch, M. Wild, and P. Tschuck, 2004: Estimating the decadal predictability of a coupled AOGCM. *J. Climate*, **17**, 4463–4472.
- , F. Sienz, and M. Latif, 2006: Influence of the multidecadal Atlantic meridional overturning circulation variability on European climate. *J. Climate*, **19**, 6062–6067.
- Rayner, N. A., D. E. Parker, E. B. Horton, C. K. Folland, L. V. Alexander, D. P. Rowell, E. C. Kent, and A. Kaplan, 2003: Global analyses of sea surface temperature, sea ice, and night marine air temperature since the late nineteenth century. *J. Geophys. Res.*, **108**, 4407, doi:10.1029/2002JD002670.
- Redi, M. H., 1982: Oceanic isopycnal mixing by coordinate rotation. *J. Phys. Oceanogr.*, **12**, 1154–1158.
- Roeckner, E., and Coauthors, 2003: The atmospheric general circulation model ECHAM5. Part I: Model description. Max-Planck-Institut für Meteorologie Rep. 349, 140 pp.
- Roemmich, D., and W. Owens, 2000: The Argo Project: Global ocean observations for understanding and prediction of climate variability. *Oceanography*, **13**, 45–50.
- Roesch, A., M. Wild, H. Gilgen, and A. Ohmura, 2001: A new snow cover fraction parameterization for the ECHAM4 GCM. *Climate Dyn.*, **17**, 933–946.
- Schulz, J.-P., L. Dümenil, and J. Polcher, 2001: On the land surface–atmosphere coupling and its impact in a single-column atmospheric model. *J. Appl. Meteor.*, **40**, 642–663.
- Smith, D. M., S. S. Cusack, A. W. Colman, C. K. Folland, G. R. Harris, and J. M. Murphy, 2007: Improved surface temperature prediction for the coming decade from a global climate model. *Science*, **317**, 796–799.
- Stammer, D., and Coauthors, 2002: Global ocean circulation during 1992–1997, estimated from ocean observations and a general circulation model. *J. Geophys. Res.*, **107**, 3118, doi:10.1029/2001JC000888.
- Tiedtke, M., 1989: A comprehensive mass flux scheme for cumulus parameterization in large-scale models. *Mon. Wea. Rev.*, **117**, 1779–1800.
- Troccoli, A., and T. N. Palmer, 2007: Ensemble decadal prediction from analysed initial conditions. *Phil. Trans. Roy. Soc.*, **365A**, 2179–2191.
- von Storch, J.-S., 2008: Toward climate prediction: Interannual predictability due to an increase in CO₂ concentration as diagnosed from an ensemble of AO GCM integrations. *J. Climate*, **21**, 4607–4628.
- Wolff, J. O., E. Maier-Reimer, and S. Legutke, 1997: The Hamburg Ocean Primitive Equation Model HOPE. Deutsches Klimarechenzentrum (DKRZ) Tech. Rep. 13, 98 pp.